Journal of the European Ceramic Society 19 (1999) 1003–1006

PII: S0955-2219(98)00362-8
0955-2219/99/$ - see front matter

# Nonisothermal Sintering of Mn Doped ZnO

Jiaping Han, A. M. R. Senos* and P. Q. Mantas

Department of Ceramic and Glass Engineering/UIMC, University of Aveiro, 3810 Aveiro, Portugal

***Abstract***

*The sintering of pure ZnO and ZnO doped with Mn, obtained by addition of $Mn(NO_3)_2.4H_2O$ in the concentration from 0·1 to 1·2 mol%, was investigated by dilatometry at constant heating rates, from 1 to 15 °C min$^{-1}$. Mn shifts the onset of the sintering towards higher temperatures, but no significant effect of the Mn doping level on the shrinkage was observed. Accordingly, the calculated activation energy for the first stage, changed from ~320 kJ mol$^{-1}$ for pure ZnO to ~440 kJ mol$^{-1}$ for Mn doped ZnO. Using classical sintering models to analyse the initial stage sintering of all the compositions, two sintering mechanisms were found to control the initial stage sintering. The first region is identified with a grain boundary sliding mechanism, while volume diffusion is the controlling mechanism in the second region. With the increase of the Mn content, the grain boundary sliding rate remains constant, but the volume diffusion rate is reduced.* © *1999 Elsevier Science Limited. All rights reserved*

*Keywords*: constant heating rate, sintering, ZnO

## 1 Introduction

Isothermal sintering has a heating-up period in which considerable microstructural development and densification can occur. Therefore, under isothermal sintering conditions, it is difficult to study the initial stage of sintering. Furthermore, large samples or large furnaces in industry can not be subjected to very high heating rates in order to minimise the heating-up period. Constant heating rate (CHR) sintering has not these disadvantages and it is particularly useful to study the initial stage of sintering.[1–3]

*To whom correspondence should be addressed. Fax: +351-34-25300; e-mail: anamor@cv.ua.pt

Some sintering equations were developed to analyse the data of CHR sintering during the initial stage. The general equation for the shrinkage rate in this stage can be written in the following form:[4]

$$\frac{\mathrm{d}Y}{\mathrm{d}t} = A_0 \frac{1}{G^m Y^n} \frac{\exp\left(-\frac{Q}{RT}\right)}{T} \tag{1}$$

where $Y = (1_0 - 1)/1$ is the linear shrinkage of the specimen, $G$ is the particle size, $Q$ is the activation energy for sintering, $R$ is the gas constant, $T$ is the absolute temperature, and $A_0$ is a constant depending only on the material parameter and on the sintering mechanism. The exponents $m$ and $n$ have the values of $m = 1$ and $n = 0$ for viscous flow, of $m = 3$ and $n = 1$ for volume diffusion and of $m = 4$ and $n = 2$ for grain boundary diffusion mechanism.

Based on eqn (1), other equations were derived to determine the sintering parameters in the initial stage under CHR conditions. The following equation was formulated by Young and Cutler:[1]

$$T^P \frac{\mathrm{d}Y}{\mathrm{d}T} = A_1 \exp\left(-\frac{Q}{(n+1)RT}\right) \tag{2}$$

where $Y$, $T$, $R$, $Q$, and $n$ have the same meaning as before. $A_1$ is a constant depending only on the material parameter and on the sintering mechanism, assuming that $G$ is approximately constant in the initial stage. The exponent $p$ has the value of 1 for viscous flow, of 3/2 for volume diffusion and of 5/3 for grain boundary diffusion mechanism.

Venkatu and Johnson[2] developed the following sintering equation:

$$CY^{n-1} = A_2 \exp\left(-\frac{Q+Q'}{RT}\right) \tag{3}$$

where $Y$, $Q$, $R$, $T$, and $n$ have the same meaning as before, $C$ is the heating rate, and $A_2$ is a constant with the same characteristics as $A_1$, in eqn (2). $Q'$

has the value of 24 kJ mol$^{-1}$ for viscous flow, and of 12 kJ mol$^{-1}$ for both volume diffusion and grain boundary diffusion mechanisms.

Based on the above sintering parameters and sintering models, the sintering kinetics of pure ZnO and Mn-doped ZnO in the initial stage are analysed and the effect of Mn addition on the sintering of ZnO is investigated in the present work.

## 2 Experimental Procedure

Reagent grade ZnO powder (Aldrich, Milwaukee, WI) with 99.9% purity and mean particle size of 0·26 $\mu$m was used. To dope with Mn, alcohol solutions of hydrated manganese nitrate ($Mn(NO_3)_2.4H_2O$) were prepared and mixed with ZnO powder, in concentrations of nitrate from 0·1 to 1·2 mol%, relatively to ZnO, in a planetary milling for 4 h. The slurry was dried and the obtained powder was calcined at 450 °C for 1 h to remove the nitrate. Cylindrical pellets with relative density of $60 \pm 1(\%)$ were obtained by isostatic pressing at 200 MPa. Constant heating rate sintering was performed at heating rates ranging from 1 to 15 °C min$^{-1}$ in air. The linear shrinkage during sintering was recorded by a computer assisted dilatometer with correction of the instrument length variation and of the thermal expansion of the sample. Particle size was measured on SEM micrographs.

## 3 Results and Discussion

The linear shrinkage of pure ZnO and of Mn-doped ZnO sintered at a constant heating rate of 5 °C min$^{-1}$ are shown in Fig. 1. The addition of Mn shifts the onset of sintering towards higher temperatures, but with the increase of the Mn content from 0·1 to 1·2%, no significant change of the onset of sintering is observed and the shrinkage curves shift slightly to higher temperatures.

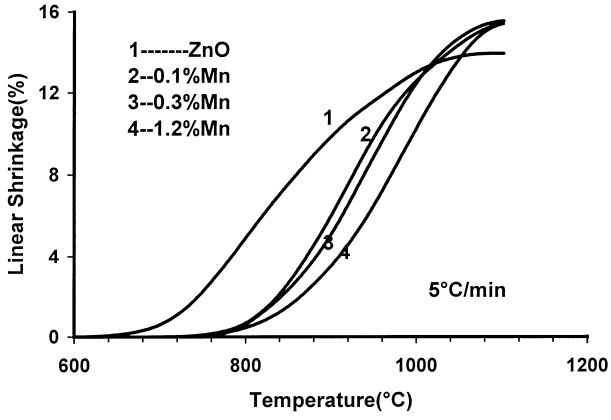


**Fig. 1.** Linear shrinkage of pure ZnO and Mn-doped ZnO compacts sintered at a constant heating rate of 5 °C min$^{-1}$.

The activation energies for sintering in the initial stage, for pure ZnO and Mn-doped ZnO, were determined according to eqns (1) and (3). Considering eqn (1), the plots of $\log(T\mathrm{d}Y/\mathrm{d}t)$ versus $1/T$ at a constant shrinkage, $Y = 1\%$, for all the compositions are shown in Fig. 2. The points at constant shrinkage in Fig. 2 were obtained for each composition by changing the heating rate from 1 to 15 °C min$^{-1}$. Grain size measurements on SEM micrographs show that the grain sizes remain practically constant ($G \simeq 0.26\ \mu m$) for linear shrinkage up to 5% in all samples. Therefore, the activation energies for the initial stage sintering can be calculated from the slopes in Fig. 2 and they are presented in Table 1. Figure 3 shows the plots of $\log(C)$ versus $1/T$ at a constant shrinkage of 1% for all compositions according to eqn (3). Considering that $Q' = 12$ kJ mol$^{-1}$ in eqn (3), we calculated the values of the activation energies from the slopes in Fig. 3, which are also shown in Table 1. For pure ZnO and Mn-doped ZnO, the activation energies calculated from eqns (1) and (3) are in good agreement and show that the value of $Q$ increases from ~320 kJ mol$^{-1}$ for pure ZnO to ~440 kJ mol$^{-1}$ for Mn-doped ZnO, independently of the Mn content. The increase of the value of the apparent activation energy by the effect of an additive is commonly observed in sintering of metal oxides[5–7] and does not necessarily mean that the kinetic controlling mechanism was changed.[6,7]

The sintering exponent n in the initial stage of pure ZnO and Mn-doped ZnO was evaluated according to eqns (1) and (2). The plots of $\log\left(T^{3/2}\mathrm{d}Y/\mathrm{d}T\right)$ versus $1/T$ at a constant heating rate of 5 °C min$^{-1}$ in the range of $Y \leq 2\%$ are shown in Fig. 4. An intermediate value of $p = 3/2$ in eqn (2) is assumed in Fig. 4, since the constant value of $p$ has no significant effect on the slope of these plots. From the plots of $\log\left(T^{3/2}\mathrm{d}Y/\mathrm{d}T\right)$ versus $1/T$ at constant heating rates from 1 to 15 °C min$^{-1}$, the average values of $Q/(n+1)$ were obtained and they are presented in Table 1. Taking

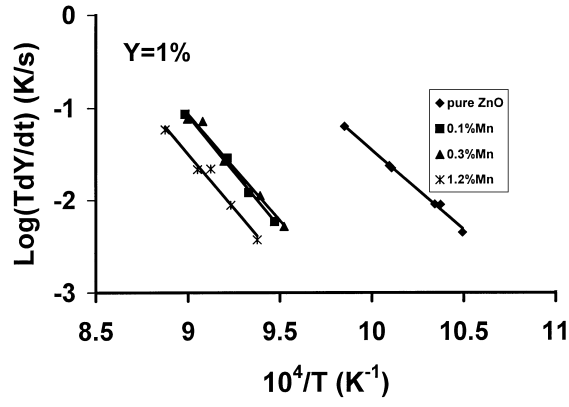


**Fig. 2.** Plots of $\log(T\mathrm{d}Y/\mathrm{d}t)$ versus $1/T$ at constant shrinkage of 1% for pure ZnO and Mn-doped ZnO.

the values of the activation energy $Q$ determined from eqns (1) and (3), $n$ can now be calculated and they are also presented in Table 1. The $n$ values are between the theoretical values of $n = 0$ for viscous flow and $n = 1$ for volume diffusion, and the trend is to increase from ~0.6 for pure ZnO and 0.1% Mn doped ZnO to ~1.2 for 1.2% Mn doped ZnO.

Figure 5 (a) and (b) show the plot of $\log(\mathrm{d}Y/\mathrm{d}t)$ versus $\log(Y)$ within the limits of the first stage($Y \leq 2\%$) for pure ZnO and Mn-doped ZnO at constant temperatures. Despite the scatter of the experimental data, two regions can be depicted for both pure and Mn-doped ZnO, corresponding to a value of $n \approx 0$ (region I) and $n \approx 1$ (region II) in eqn (1). The value of $n = 0$ in region I is identified with a viscous flow mechanism, which may dominate the beginning of sintering, although no liquid phase was detected in the microstructural observations, while the value of $n = 1$ in region II indicates that shape accommodation governed by volume diffusion seems to be the controlling mechanism. This type of kinetics in region I has been often found in solid state sintering of pure and doped ZnO.[8–10,13,14] and other oxides of fine powders like NiO,[9] $TiO_2$,[11,12], $Al_2O_3$[11,12], or MgO[13] and has been interpreted as a grain boundary sliding mechanism, dominating the densification as long as the grain boundary sliding rate is lower than the shape accommodation rate.[9,10,14] It can be observed in Fig. 5(b) that the amount of Mn has no effect on the grain boundary sliding rate (region I), while it slightly reduces the shape accommodation rate (region II), leading to a decrease of the extent of the region I for higher Mn doping levels. When the mn content increases from 0·1 to 1·2%, the observed constant shrinkage rate in region I (at the beginning of sintering) is in agreement with the observation of no change of the onset of the shrinkage in Fig. 1. On the other hand, with the increasing of Mn doping level, the increase of the exponent $p$ from

**Table 1.** Sintering activation energies $Q$ and sintering exponent $n$ of pure ZnO and Mn-doped ZnO

| *Composition* | Q *(kJ mol$^{-1}$) [from eqn (1)]* | Q *(kJ mol$^{-1}$) [from eqn (3)]* | Q/(n+1) *(kJ mol$^{-1}$) [from eqn (2)]* | n |
|---|---|---|---|---|
| Pure ZnO | 329 ± 4 | 316 ± 5 | 200 ± 7 | 0·6 |
| ZnO + 0·1% Mn | 449 ± 16 | 453 ± 6 | 279 ± 9 | 0·6 |
| ZnO + 0·3% Mn | 437 ± 5 | 437 ± 3 | 247 ± 21 | 0·8 |
| ZnO + 1·2% Mn | 447 ± 8 | 437 ± 10 | 201 ± 19 | 1·2 |

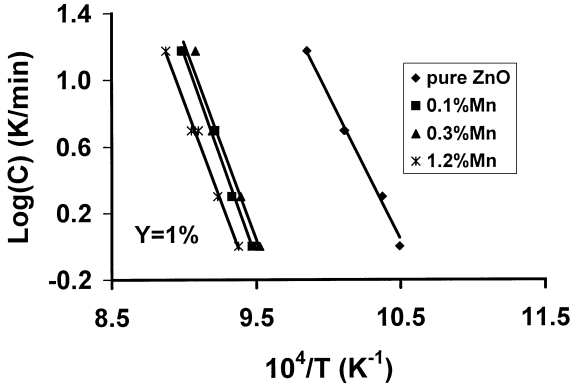


**Fig. 3.** Plots of $\log(C)$ versus $1/T$ at constant shrinkage of 1% for pure ZnO and Mn-doped ZnO.

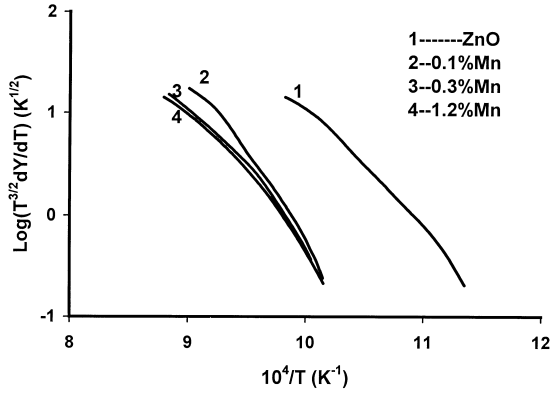


**Fig. 4.** Plots of $\log(T^{3/2}\mathrm{d}Y/\mathrm{d}T)$ versus $1/T$ at constant heating rate of 5 °C in the range of $Y \leq 2\%$.

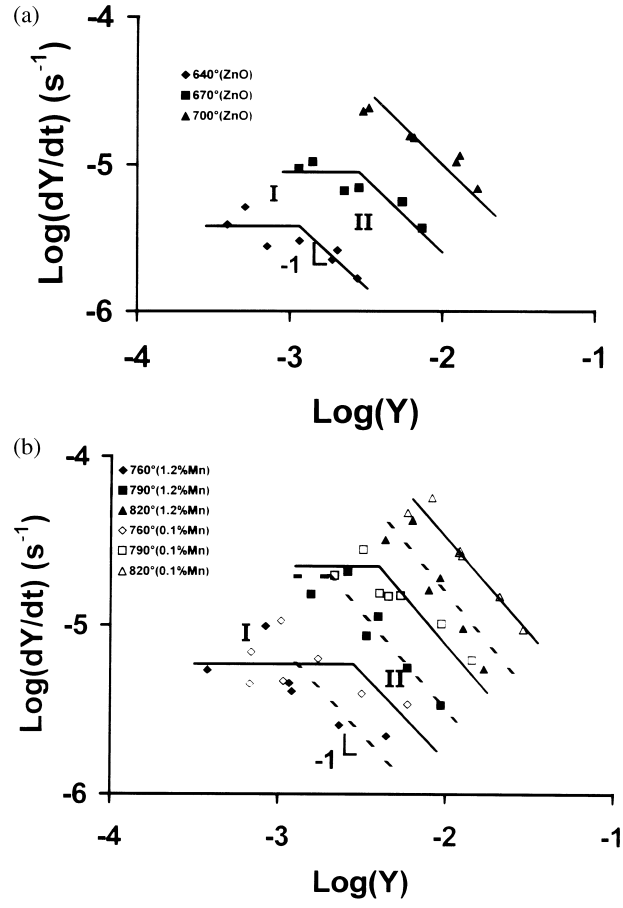


**Fig. 5.** Plots of $\log(\mathrm{d}Y/\mathrm{d}t)$ versus $\log(Y)$ at constant temperatures for pure ZnO and Mn-doped ZnO: (a) pure ZnO; (b) Mn-doped ZnO.

0·6 to 1·2 is also related to the decrease of the extent of region I and to the enlargement of region II. This kinetic analysis suggests that the structure of the grain boundaries is not affected by Mn contents higher than 0·1% at least in the beginning of the sintering process, but an accurate observation of the structure and chemical composition of the grain boundaries and of the surfaces must be performed in order to have a better understanding of the effect of Mn on the sintering of ZnO.

## 4 Conclusion

Using CHR techniques to analyse the initial-stage sintering of pure and Mn-doped ZnO, two sintering mechanisms were found to control the initial stage sintering for all the compositions studied. The first region is identified with a grain boundary sliding mechanism, while a volume diffusion mechanism dominates the kinetics of the second region. When the Mn content increases from 0·1 to 1·2 mol%, the grain boundary sliding rate remains constant, but the volume diffusion rate is reduced. Coincidentally, the onset of the shrinkage is not changed, but the extent of the second region is enlarged. These results suggest that, in the Mn content ranging from 0·1 to 1·2 mol%, the structure of ZnO grain boundaries is not affected by the presence of Mn during the initial stage of sintering.

## Acknowledgements

The author (Jiaping Han) would like to acknowledge the financial support of Praxis XXI, JNICT, Portugal.

## References

1. Young, W. S. and Cutler, I. B., Initial sintering with constant rates of heating. *J. Am. Ceram. Soc.*, 1970, **53**(12), 659–663.
2. Venkatu, D. A. and Johnson, D. L., Analysis of sintering equations pertaining to constant rates of heating. *J. Am. Ceram. Soc.*, 1972, **55**, 383–385.
3. Woolfrey, J. L. and Bannister, M. J., Nonisothermal techniques for studying initial-stage sintering. *J. Am. Ceram. Soc.*, 1972, **55**(8), 390–394.
4. Johnson, D. L., New method of obtaining volume, grain-boundary, and surface diffusion coefficients from sintering data. *J. Appl. Phys.*, 1969, **40**(1), 192–200.
5. Keski, J. R. and Cutler, I. B., Initial sintering of $Mn_xO$-$Al_2O_3$. *J. Am. Ceram. Soc.*, 1968, **51**(8), 440–444.
6. Brook, R. J., Effect of $TiO_2$ on the initial sintering of $Al_2O_3$. *J. Am. Ceram. Soc.*, 1972, **55**(2), 114–115.
7. Hollenberg, G. W. and Gordon, R. S., Origin of anomalously high activation energies in sintering and creep of impure refractory oxides. *J. Am. Ceram. Soc.*, 1973, **56**(2), 109–110.
8. Moriyoshi, Y. and Komatsu, W., Kinetics of initial sintering with grain growth. *J. Am. Ceram. Soc.*, 1970, **53**(12), 671–675.
9. Senos, A. M. R., Santos, M. R., Moreira, A. P. and Vieira, J. M., Grain boundary phenomena in the early stages of sintering of MO oxides. In *Surfaces and Interfaces of Ceramic Materials*, ed. L. C. Dufour, C. Monty and G. Petot-Ervas, NATO ASI Series. Kluwer Academic Publishers, London, 1989, pp. 553–556.
10. Senos, A. M. R. and Vieira, J. M., Pore size distribution and particle rearrangement during sintering. In Proceedings of the International Conference *Third Euro-Ceramics*, Vol. 1, ed. P. Duran and J. F. Fernandez, Faenza Editrice Iberica S. L., Faenza, Italy, 1993, pp. 821–826.
11. Vergnon, P. G., Juillet, F. E. and Teichner, S. J., Sintering of ultrafine particles of anatase and delta alumina. *Sci. Ceram.*, 1970, **5**, 47–62.
12. Vergnon, P. G., Astier, M. P., Beruto, D., Brula, G. and Teichner, S. J., Frittage des solides très finement divisés. *Rev. Int. Hautes Temper. et Refract.*, 1972, **9**, 271–278.
13. Varela, J. A., Structural rearrangement during sintering of MgO. *J. Am. Ceram. Soc.*, 1983, **66**, 77–82.
14. Senos, A. M. R., Sintering kinetics in open porosity stages of zinc oxide, Ph. D. Thesis, University of Aveiro, Aveiro, Portugal, 1993.